

**Molecular-Recognition Characteristics of SAM-Binding Riboswitches\*\***

*Jinsoo Lim, Wade C. Winkler, Shingo Nakamura, Valerie Scott, and Ronald R. Breaker\**

Riboswitches are highly structured domains that typically reside within noncoding regions of certain messenger RNAs (mRNAs).<sup>[1]</sup> These RNAs are genetic control elements that monitor the level of specific metabolites by selective binding without the need for intermediary protein factors. Metabolite binding controls gene expression by several different mechanisms that involve allosteric changes in RNA folding. Riboswitches typically consist of two functional domains, an aptamer domain and an expression platform, which respectively bind metabolite and trigger gene-expression changes. A number of riboswitch classes have been discovered that recognize a variety of important compounds, such as coenzymes, amino acids, and nucleobases, thus indicating that these metabolite-sensing RNAs serve as important components of genetic control circuitry in some organisms.<sup>[2]</sup> An understanding of the interactions between riboswitches and their metabolite ligands should provide greater insight into the capabilities of RNA as a genetic switch. Furthermore, this knowledge might empower future efforts to design novel antimetabolites that bind to riboswitches, inhibit the expression of key metabolic genes, and thus be selectively toxic to bacteria that carry these RNAs.<sup>[3]</sup>

S-adenosyl-L-methionine (SAM; **1**; Figure 1) is an important enzyme cofactor in many biosynthetic pathways.<sup>[4]</sup> In bacteria of the *Bacillus/Clostridium* group, SAM-binding riboswitches (SAM-I; originally termed “S-box” RNAs)<sup>[5]</sup> control multiple different genes involved in SAM biosynthe-

[\*] Dr. J. Lim, V. Scott, Prof. R. R. Breaker  
Department of Molecular, Cellular, and Developmental Biology  
Yale University  
New Haven, CT 06520 (USA)  
Fax: (+1) 203-432-0753  
E-mail: ronald.breaker@yale.edu

Dr. W. C. Winkler  
Department of Biochemistry  
University of Texas Southwestern Medical Center at Dallas  
Dallas, TX 75390 (USA)

Dr. S. Nakamura  
Takeda Pharmaceutical Co. Ltd.  
Chuo-ku, Osaka 540-8645 (Japan)

[\*\*] We thank Prof. G. Michael Blackburn (University of Sheffield) for generous gifts of compounds **5** and **6** and Dr. Gail Emilsson and other members of the Breaker laboratory for helpful comments. This study was supported by the grants from the US National Institutes of Health, the US National Science Foundation, DARPA, and the David and Lucile Packard Foundation. SAM = S-adenosyl-methionine.



Supporting information for this article is available on the WWW under <http://www.angewandte.org> or from the author.

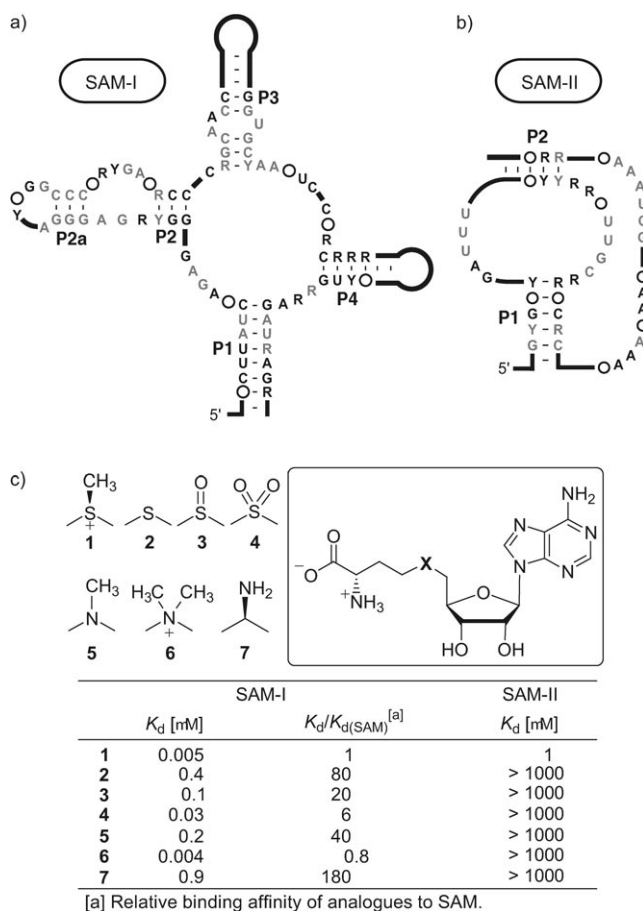


**Figure 1.** Consensus sequence and structure for a) aptamers of SAM-I riboswitches found in Gram-positive bacteria and b) aptamers of the SAM-II riboswitches found in alpha proteobacteria. The black and gray letters denote nucleotides that are conserved in 80 and 95%, respectively, of the representatives identified.<sup>[6,7]</sup> c) Molecular recognition of SAM and its analogues by the SAM-I and -II motifs.

sis, amino acid biosynthesis, and the general metabolism of sulfur.<sup>[6]</sup> More recently,<sup>[7]</sup> we have identified a second class of SAM-dependent riboswitches (SAM-II) in alpha proteobacteria. Representatives of this riboswitch class have sequence and structural elements that are distinct from SAM-I riboswitches even though they control genes involved in similar metabolic processes. The existence of two distinct riboswitch classes for SAM provides the first opportunity to compare the molecular-recognition capabilities of two natural aptamers for the same ligand.

Herein, we established the molecular-recognition characteristics of the aptamer domain of a SAM-I riboswitch from the *yitJ* gene of *Bacillus subtilis*.<sup>[6c]</sup> This data is compared with the molecular-recognition characteristics of a SAM-II riboswitch aptamer from the *metA* gene of *Agrobacterium tumefaciens*.<sup>[7]</sup> We conclude from these results that the two RNAs indeed form distinct binding pockets for SAM. However, both classes of SAM riboswitches strongly discriminate against most analogues of SAM, which is a requisite for any metabolite-binding receptor that serves as a precision gene-control element.

To uncover determinants of molecular recognition for these RNAs, a series of thioether-modified SAM analogues were tested for their ability to serve as ligands (Figure 1).<sup>[8]</sup> Values for the dissociation constant ( $K_d$ ) were determined by conducting in-line probing assays<sup>[9,10]</sup> in the presence of various concentrations of ligand (Figure 2). These assays can be used to establish the apparent dissociation constant for RNA–ligand complexes. As reported earlier,<sup>[6c]</sup> **2**, which lacks both a methyl group and the positive charge at the sulfur atom, loses affinity for the SAM-I motif by a factor of 80. In contrast, sulfoxide **3** and sulfone **4** derivatives,<sup>[11]</sup> although lacking the methyl group, are far better ligands for SAM-I relative to **2**. For example, SAM is bound by the SAM-I motif only sixfold better than **4**. The aza analogue<sup>[12]</sup> of SAM (**5**) is more isosteric but largely uncharged under in-line probing-assay conditions<sup>[13]</sup> and therefore is more similar to **2**. Furthermore, sinefungin **7**, a SAM isoster with the same chirality as SAM, drops by more than two orders of magnitude in affinity. The most potent ligand for SAM-I is an aza analogue<sup>[12]</sup> of SAM (**6**) that carries an extra methyl group and a higher positive charge density.

We conclude that SAM-I RNAs are unlikely to require the methyl group or a specific stereochemistry of the thioether for binding. Moreover, the net positive charge density at the sulfur atom appears to be a key recognition determinant for SAM-I RNAs. This position might form an electrostatic interaction with an anionic or electronegative group of the RNA.

This charge-density correlation is supported by the chemical shifts of both H5' and Hγ in the <sup>1</sup>H NMR spectrum (Figure 3). As the thioether region is located in between H5' and Hγ, the alteration of electron density at this position influences the chemical shifts of the protons.<sup>[12,14]</sup> When compared with **2**, the chemical shift of ribose proton H5' for **1**, **4**, and **6** shifts downfield from  $\delta = 0.94$  to 0.98 ppm, thus suggesting that the net charge densities of these analogues are highly positive.<sup>[15]</sup> The extent of the difference in the chemical shift of the Hγ proton for the derivatives is also similar to that of H5' (from  $\delta = 0.91$  to 1.00 ppm).

The SAM-II motif exclusively binds SAM in contrast to SAM-I and rejects even those compounds that are most tightly bound by SAM-I, such as **4** and **6**.<sup>[7]</sup> This behavior suggests that the positive charge and the methyl group of SAM might both be critical for molecular recognition by SAM-II RNAs. Moreover, the dramatic difference in the binding affinity of **6** between the two aptamer classes implies that the extra methyl group sterically interferes with binding such that other contacts that exist between SAM-II and its ligand are offset.

Subsequent to the discovery of the potent activity of **4**, we further synthesized<sup>[8]</sup> a complete set of analogues of **4**, in which one of the heteroatoms is systematically eliminated or altered to a carbon atom while the remaining functional groups are kept intact. The SAM analogues were prepared from 5'-chloro-5'-deoxyadenosine derivatives,<sup>[16]</sup> which were converted into S-adenosyl-L-homocysteine analogues by the reaction with the L-homocysteine disodium salt.<sup>[17]</sup> Oxidation of S-adenosyl-L-homocysteine analogues with a molybdate

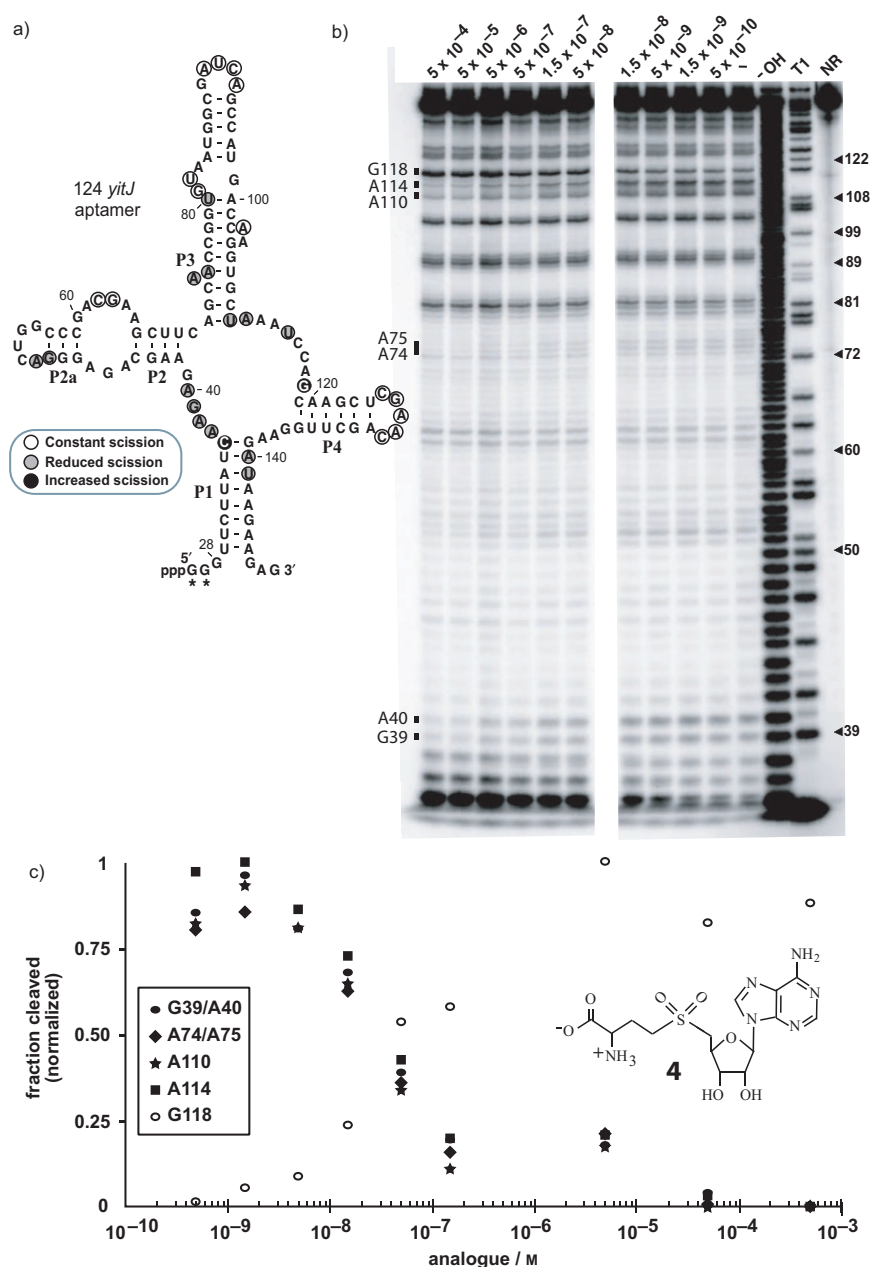


**Figure 2.** SAM-I riboswitches and a representative in-line probing assay using 124 *yitJ* RNA from *B. subtilis* and various concentrations of SAM. a) Sequence and secondary-structure model of the *yitJ* SAM-I aptamer. P1–P4 identify conserved base-pairing elements. Unshaded, encircled nucleotides indicate a putative pseudo knot interaction. Nucleotide 1 corresponds to the putative transcriptional start site. Asterisks identify nucleotides that were added to the construct to permit efficient transcription in vitro. The first nucleotide of the AUG start codon is 235 (not shown). Sites of structural modulation upon introduction of SAM are depicted as described. b) Spontaneous cleavage patterns of 124 *yitJ* in the absence (–) or presence of SAM at the molar concentrations indicated were examined after separation by polyacrylamide gel electrophoresis. NR = no reaction, T1 = partial digest with RNase T1, <sup>−</sup>OH = partial digest with alkali, respectively. Certain fragment bands corresponding to digestion by T1 (which cleaves after guanine residues) are depicted. Bars identify positions of substantial modulation of spontaneous cleavage that were used for quantification (see the Experimental Section). c) Plot of the normalized fraction of 124 *yitJ* RNA cleaved at each site designated versus the concentration of the sulfone analogue 4 of SAM. Half-maximum change in spontaneous cleavage occurs at a concentration of 4 of approximately 50 nM, which reflects the apparent  $K_d$  value of this ligand with the *yitJ* aptamer.

solution containing hydrogen peroxide yielded **8–18** (Table 1).<sup>[11]</sup>

As SAM-II rejects **4**, all the synthesized sulfone analogues were not expected to bind significantly to the SAM-II motif, and thus they were tested only with SAM-I. The amino acid modified analogues, devoid of amine or carboxylic acid groups (**9** and **10**, respectively), had no detectable binding to SAM-I, thus implying that the amino acid might form strong electrostatic or hydrogen-bonding interactions with the RNA. By examining sugar-modified analogues, the 3'-hydroxy group appears to be less important than the 2'-hydroxy group (**13** and **12**, respectively). The 6-amino group of adenine is so important that replacement by either a hydroxy group or a hydrogen atom (**15** and **14**, respectively) is not tolerated. The 7-aza group is likely to be critical for hydrogen bonding, whereas the 3-aza group is less important than any other amine in the adenine ring (**16** and **17**, respectively). An extra amino group at the 2-position of adenine (**18**) decreases binding by a factor of 67, thus suggesting a tight pocket is formed in this case.

In summary, we have examined and compared the molecular-recognition characteristics of both the SAM-I and -II aptamers (Scheme 1) by using in-line probing assays with a series of SAM analogues. The 6-amino, 7-aza, and 2'-hydroxy groups of the nucleobase, and the functional groups on the amino acid moiety of SAM appear to participate in molecular recognition with SAM-I. However, SAM-II is far more selective for the thioether linkage of SAM, and therefore a different analogue set was used to further establish other molecular determinants for this RNA.<sup>[7]</sup> The fact that each riboswitch has different substrate-recognition determinants confirms that their sequence and structural differences form distinct binding pockets for SAM. Furthermore, there appears to be considerable opportunity to design novel SAM analogues that selectively trigger SAM-I riboswitches, perhaps without risk of interacting with other SAM-binding biopolymers. Given that SAM-I riboswitches in Gram-positive organisms control numerous genes whose products participate in fundamental metabolic pathways, such SAM analogues might find application as antibiotic compounds that selectively inhibit bacterial growth.

## Experimental Section

The aptamer domain from the SAM-I riboswitch of the *yitJ* gene from *B. subtilis* (Figure 2a) was generated as described previously.<sup>[6c]</sup> 5'-<sup>32</sup>P-Labeled

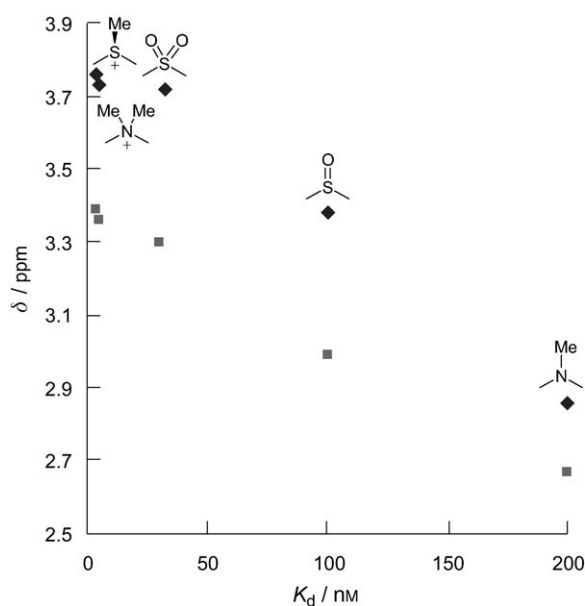
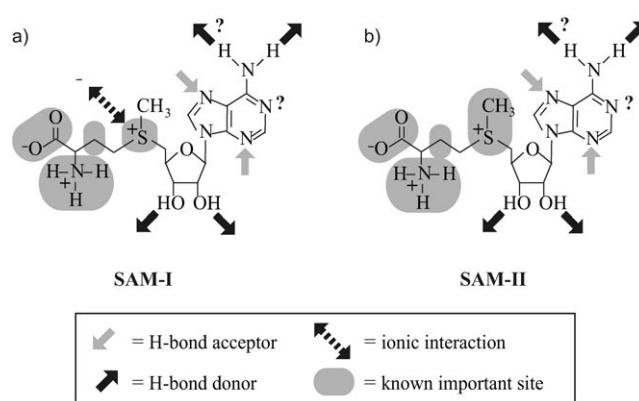


**Figure 3.** Charge-density correlation plot. Binding affinities ( $K_d$ ) of analogues are inversely proportional to the chemical shifts of the protons H5' (diamonds) and H $\gamma$  (squares) of the corresponding derivatives.

RNA was prepared using calf intestinal phosphatase (Roche Diagnostics), T4 polynucleotide kinase (New England Biolabs), and [ $\gamma$ - $^{32}$ P]ATP (Amersham Biosciences) according to the manufacturer's directions and purified by polyacrylamide gel electrophoresis. Similarly, radiolabeled RNAs that represent the SAM-II riboswitch aptamer for the *metA* gene from *A. tumefaciens* were prepared. Genomic DNA used to prepare the template for transcription of the SAM-II construct<sup>[7]</sup> was obtained from *Agrobacterium tumefaciens* strain GV2260 (a gift from the S. Dinesh-Kumar Lab, Yale University). For each probing reaction, approximately 1 nM 5'- $^{32}$ P-labeled RNA was incubated for about 40 h at 25 °C in 50 mM Tris-HCl (pH 8.3 at 25 °C), 20 mM MgCl<sub>2</sub>, 100 mM KCl, with added compounds as indicated for each experiment. Additional experimental details are similar to those described elsewhere.<sup>[2a-b]</sup> Polyacrylamide gels that separate the RNA cleavage products from in-line probing assays were



**Scheme 1.** Predicted molecular-recognition determinants of SAM riboswitches. The schematic representation reflects a possible pattern of molecular interactions between SAM and a) the aptamer domain of SAM-I riboswitches and b) the aptamer domain of SAM-II riboswitches. Note that, in some cases, the precise type of molecular contact or the number of contacts for a given functional group cannot be determined from the limited data currently available. Shading on the hydrocarbon side chain of the methionyl moiety reflects the importance of length. Also the molecular-recognition patterns are likely incomplete for both aptamer classes. A more comprehensive assessment of the contacts between SAM-II RNA and its ligand will require the use of analogues that retain the natural methylated thioether linkage, and the design of tight-binding analogues would be greatly aided by an atomic-resolution structure of the RNA bound to SAM.

scanned and quantitated using a molecular dynamics STORM 820 PhosphorImager system. The  $K_d$  value of 124  $\mu$ M for SAM and for each SAM analogue was determined by plotting the normalized fraction of RNA cleaved at six regions (e.g., Figure 2c) versus the logarithm of the concentration of SAM in molar units. The concentration of SAM needed to induce half-maximum change in RNA-cleavage extent was interpreted as the apparent  $K_d$  value. Similar data for the SAM-II 164 *metA* RNA is reported elsewhere.<sup>[7]</sup>

Received: September 8, 2005  
Published online: December 28, 2005

**Table 1:** Dissociation constant ( $K_d$ ) values for SAM analogues with the *yitJ* SAM-I riboswitch aptamer from *B. subtilis*.

	R <sup>1</sup>	R <sup>2</sup>	R <sup>3</sup>	R <sup>4</sup>	R <sup>5</sup>	W	X	Y	Z	$K_d$ [ $\mu$ M]
<b>4</b>	NH <sub>2</sub>	CO <sub>2</sub> H	H	OH	OH	NH <sub>2</sub>	N	N	H	$3 \times 10^{-2}$
<b>8</b>	H	CH <sub>2</sub> OH	H	OH	OH	NH <sub>2</sub>	N	N	H	> 1000
<b>9</b>	H	CO <sub>2</sub> H	H	OH	OH	NH <sub>2</sub>	N	N	H	> 1000
<b>10</b>	NH <sub>2</sub>	H	H	OH	OH	NH <sub>2</sub>	N	N	H	> 1000
<b>11</b>	NH <sub>2</sub>	CO <sub>2</sub> H	OH	H	OH	NH <sub>2</sub>	N	N	H	40
<b>12</b>	NH <sub>2</sub>	CO <sub>2</sub> H	H	H	OH	NH <sub>2</sub>	N	N	H	30
<b>13</b>	NH <sub>2</sub>	CO <sub>2</sub> H	H	OH	H	NH <sub>2</sub>	N	N	H	5
<b>14</b>	NH <sub>2</sub>	CO <sub>2</sub> H	H	OH	OH	H	N	N	H	> 1000
<b>15</b>	NH <sub>2</sub>	CO <sub>2</sub> H	H	OH	OH	OH	N	N	H	> 1000
<b>16</b>	NH <sub>2</sub>	CO <sub>2</sub> H	H	OH	OH	NH <sub>2</sub>	CH	N	H	> 1000
<b>17</b>	NH <sub>2</sub>	CO <sub>2</sub> H	H	OH	OH	NH <sub>2</sub>	N	CH	H	3
<b>18</b>	NH <sub>2</sub>	CO <sub>2</sub> H	H	OH	OH	NH <sub>2</sub>	N	N	NH <sub>2</sub>	2

**Keywords:** aptamers · molecular recognition · riboswitches · RNA · structure–activity relationships

- [1] a) E. C. Lai, *Curr. Biol.* **2003**, *13*, R285–R291; b) M. Mandal, R. R. Breaker, *Nat. Rev. Mol. Cell Biol.* **2004**, *5*, 451–463.
- [2] a) A. Nahvi, N. Sudarsan, M. S. Ebert, X. Zou, K. L. Brown, R. R. Breaker, *Chem. Biol.* **2002**, *9*, 1043–1049; b) W. Winkler, A. Nahvi, R. R. Breaker, *Nature* **2002**, *419*, 952–956; c) A. S. Mironov, I. Gusarov, R. Rafikov, L. E. Lopez, K. Shatalin, R. A. Krenneva, D. A. Perumov, E. Nudler, *Cell* **2002**, *111*, 747–756; d) M. Mandal, B. Boese, J. E. Barrick, W. C. Winkler, R. R. Breaker, *Cell* **2003**, *113*, 577–586.
- [3] a) J. Gallego, G. Varani, *Acc. Chem. Res.* **2001**, *34*, 836–843; b) T. Hermann, *Biopolymers* **2003**, *70*, 4–18; c) G. J. R. Zaman, P. J. A. Michiels, C. A. A. van Boeckel, *Drug Discovery Today* **2003**, *8*, 297–306.
- [4] a) H. L. Schubert, R. M. Blumenthal, X. Cheng, *Trends Biochem. Sci.* **2003**, *28*, 329–335; b) M. Fontecave, M. Atta, E. Mulliez, *Trends Biochem. Sci.* **2004**, *29*, 243–249; c) J. T. Jarrett, *Curr. Opin. Chem. Biol.* **2003**, *7*, 174–182; d) P. A. Frey, O. T. Magnusson, *Chem. Rev.* **2003**, *103*, 2129–2148; e) J. L. Martin, F. M. McMillan, *Curr. Opin. Struct. Biol.* **2002**, *12*, 783–793.
- [5] F. J. Grundy, T. M. Henkin, *Mol. Microbiol.* **1998**, *30*, 737–749.
- [6] a) B. A. M. McDaniel, F. J. Grundy, I. Artsimovitch, T. M. Henkin, *Proc. Natl. Acad. Sci. USA* **2003**, *100*, 3083–3088; b) V. Epshtein, A. S. Mironov, E. Nudler, *Proc. Natl. Acad. Sci. USA* **2003**, *100*, 5052–5056; c) W. C. Winkler, A. Nahvi, N. Sudarsan, J. E. Barrick, R. R. Breaker, *Nat. Struct. Biol.* **2003**, *10*, 701–707.
- [7] K. A. Corbino, J. E. Barrick, J. Lim, R. Welz, B. J. Tucker, I. Puskarz, M. Mandal, N. D. Rudnick, R. R. Breaker, *Genome Biol.* **2005**, *6*, R70.
- [8] Additional experimental and synthetic details are presented in the Supporting Information.
- [9] G. A. Soukup, R. R. Breaker, *RNA* **1999**, *5*, 1308–1325.
- [10] The rate of spontaneous cleavage of RNA by transesterification is affected by the position of the attacking nucleophile (2'-O) relative to the leaving group (5'-O); see F. H. Westheimer, *Acc. Chem. Res.* **1968**, *1*, 70–78. Changes in RNA shape, brought about by ligand binding thus change the pattern of RNA-cleavage products; see G. A. Soukup, E. C. DeRose, M. Koizumi, R. R. Breaker, *RNA* **2001**, *7*, 524–536.
- [11] R. T. Borchardt, Y. S. Wu, *J. Med. Chem.* **1974**, *17*, 862–868.
- [12] The profile of the  $pK_a$  values of **5** and  $^1\text{H}$  NMR spectroscopic data of **5** and **6** are shown in M. J. Thompson, A. Mekhalfia, D. P. Hornby, G. M. Blackburn, *J. Org. Chem.* **1999**, *64*, 7467–7473.
- [13] In-line probing used 50 mM Tris–HCl (pH 8.3 at 25 °C), 20 mM  $\text{MgCl}_2$ , 100 mM KCl, and typically 10 nM to 10 mM ligand.
- [14] The  $^1\text{H}$  NMR spectroscopic data of **3** and **4** is available in the Supporting Information and that of **1** and **2** are shown in M. L. Stolowitz, M. J. Minch, *J. Am. Chem. Soc.* **1981**, *103*, 6015–6019.
- [15] The net ionic charge of sulfur derivatives were estimated as follows:  $(\text{CH}_3)_3\text{S}^+\text{I}^-$ , +0.749 D;  $(\text{CH}_3)_2\text{S}$ , –1.608 D;  $(\text{CH}_3)_2\text{SO}$ , –0.514 D;  $(\text{CH}_3)_2\text{SO}_2$ , +0.311 D; J. Jullien, H. Stahl-Larivière, A. Trautmann, *Bull. Soc. Chim. Fr.* **1966**, 2398–2399.
- [16] M. J. Robins, F. Hansske, S. F. Wnuk, T. Kanai, *Can. J. Chem.* **1991**, *69*, 1468–1474.
- [17] R. W. Miles, L. P. C. Nielson, G. J. Ewing, D. Yin, R. T. Borchardt, M. J. Robins, *J. Org. Chem.* **2002**, *67*, 8258–8260.